2005-01-1688

# Development of a Heat Resistant Cast Iron Alloy for Engine Exhaust Manifolds

**Sung Hwan Park, Jong Moon Kim, Hak Jin Kim, Se Jin Ko, Hyoun Soo Park and Jong Dae Lim**
Hyundai Motor Company

61

## ABSTRACT

A new heat-resistant cast iron alloy has been developed for the exhaust manifolds of new passenger-car diesel engines. This development occurred because operating demands on exhaust manifolds have increased significantly over the past decade. These demands are due to higher exhaust gas temperatures resulting from tighter emission requirements, improved fuel efficiencies, and designs for higher specific engine power. These factors have led to much higher elevated temperature strength and oxidation resistance requirements on exhaust manifold alloys. Additionally, thermal fatigue that occurs directly as a result of thermal expansions and mechanical constraint has become an increasingly important issue.

The research detailed in this paper focused on the optimization of the chemical composition of a Si-Mo ductile iron to improve the mechanical and physical properties for use in an engine exhaust manifold. Low cycle fatigue and high temperature oxidation properties were evaluated and found to yield an improved alloy for exhaust manifold applications.

## INTRODUCTION

Two of the fundamental issues in the design of manifolds are how to minimize the thermal stresses and the thermal deformation. In operation, high-temperature combustion gases flow past the inner wall of the manifold. Thus, the part is subjected to cyclic thermal loads as the engine heats up and cools down as it is started and stopped.

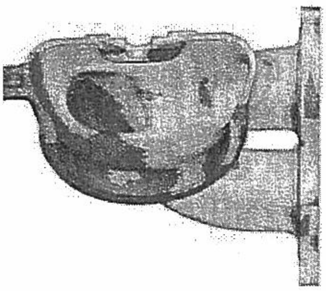

**Fig.1 - FEM Simulation Results In A Heated Manifold**

Fig. 1 shows the finite element simulation results for the stress distribution caused by thermal expansion when the manifold is heated. Over time, repeated thermal stresses cause localized plastic strains to build up in the manifold. These strains eventually adversely affect the lifetime of the manifold due to the fatigue cracks that develop.

In terms of alloys, the development trends for exhaust manifold alloys have focused on heat-resistant cast irons and on Stainless Steels. Cast irons have been a common manifold material for many years. A wide variety of microstructures are present in cast irons, including those with different free graphite types like flake, compacted, and nodular. To meet the requirements for high output engines, special heat-resistant ductile irons like Si-Mo ductile and Ni-Resist have been developed. Through the addition of elements like Si, Mo, and Ni, the high temperature strength and scaling resistance are significantly improved. Stainless steel alloys have also been selected for elevated temperature applications because of their excellent strength and resistance to oxidation and corrosion. Manifolds created from stainless steel alloys can be both cast and wrought.

Table 1 shows typical maximum use temperatures for manifolds created using a number of common alloys. In design, the target temperature of the manifold material is about 100 °C below the maximum use temperature.

High Silicon Ductile Irons have good physical properties, high scaling resistance, and low thermal expansion coefficients. However, High Silicon Ductile Irons are somewhat limited in use at high temperatures because of their low strengths.

**Table 1: Maximum Use Temperature For Various Exhaust Manifold Alloys [1]**

| Exhaust Manifold Alloy | Maximum allowable temperature in use |
|---|---|
| High Silicon Ductile Iron | 810°C |
| Si-Mo Ductile Iron | 860°C |
| Ni-Resist | 870°C |
| Wrought Stainless Steel | 920°C |
| Cast Stainless Steel | 980°C |

For the Si-Mo Ductile Irons, it is the molybdenum, added in small amounts that increase the high temperature tensile strength. A number of different types of Si-Mo alloys have been developed by varying the amounts of Silicon and Molybdenum [1]. Among these alloys, the best one is a 4% silicon, 0.8% molybdenum alloy.

## EXPERIMENTAL PROCEDURES

In this paper, we provide a detailed examination of an improved Si-Mo ductile iron that was optimized to have the best mechanical and physical properties at high temperature. The thermal expansion of the new Si-Mo ductile iron alloy and the current Si-Mo ductile iron alloy were measured by dilatometer and were calculated by Thermo-Calc to determine the $A_1$ temperature of those alloys. Phase transformation to austenite above the $A_1$ temperature increases the thermal stresses and thermal deformations of the manifold because of a high coefficient of thermal expansion (~40% more than that in ferrite).

To evaluate the scaling resistance of new alloy, high temperature oxidation tests were performed at 650~850°C in an air environment and compared to those performed on the current alloy. To determine the maximum useful temperature of new alloy, high temperature tensile tests were conducted at seven different temperatures. Hardness profiles were also measured after completion of a 300–hour oxidation test. Low cycle fatigue tests were conducted to evaluate thermal fatigue behavior of the new alloy. The plastic strain range and hysteresis loop energy of the new alloy was then compared to that of current alloy.

## RESULTS AND DISCUSSION

### ALLOY DESIGN

### Theoretical Background

Silicon enhances the performance of ductile Iron at elevated temperatures by stabilizing the ferrite matrix and forming a silicon-rich surface layer that inhibits oxidation. As Figure 2 shows, the protection from oxidation increases with increasing silicon content. Silicon levels above 4% are sufficient to prevent any significant weight gain after the formation of an initial oxide layer [2].

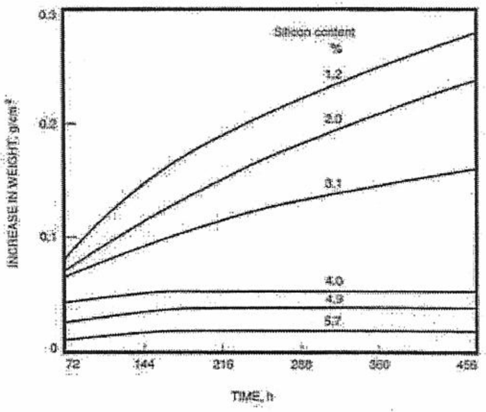

**Fig. 2 - The Effect Of Silicon On Oxidation Of A Ferritic Ductile Iron At 650°C [2]**

Silicon influences the room temperature mechanical properties of ductile Iron through solid solution hardening of the ferrite matrix. For silicon levels above 5%, the material may become too brittle for engineering applications requiring any degree of toughness (Fig. 3).

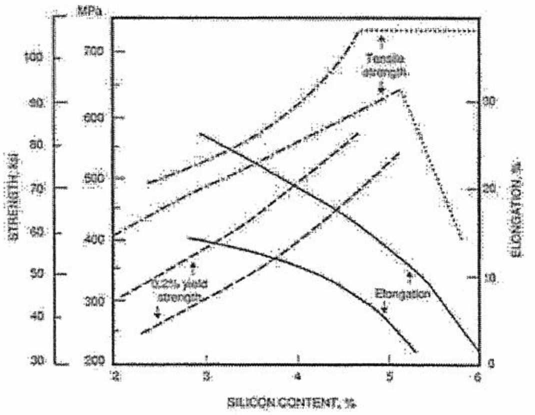

**Fig. 3 – The Effect Of Silicon On The Mechanical Properties Of A Ferritic Ductile Iron At Room Temperatures [2]**

Thus, the best combinations of oxidation resistance and mechanical properties are provided by silicon contents in the range of 4 - 5%.

Molybdenum contents of up to 1% are often used in the Si-Mo ductile irons. Increasing the molybdenum level up to 1% will enhance high temperature strength and creep resistance. However, this can reduce toughness by the formation of grain boundary carbides. Also, shrinkage defects may be increased because of the exhaustion of carbon in the melt by the formation of eutectic Mo-carbides. To ensure a carbide-free ferritic matrix, other pearlite- and carbide-stabilizing elements should be kept as low as possible.

Carbon levels in the Si-Mo ductile irons should be kept within the range of 2.8 - 3.7 wt%. The carbon content should be reduced as the silicon level is increased in accordance with the following equation:

$$C.E = \%C + \%Si/3$$

Alloy Selection

From the above theoretical background, we determined the optimum chemical composition range of the new Si-Mo ductile iron alloy to be that shown in Table 2.

**Table 2: Chemical Compositions Of The Ductile Iron Alloys (Wt %)**

| Element | C | Si | Mn | Mo |
|---|---|---|---|---|
| Current Si-Mo Alloy | 3.3-3.8 | 3.4-3.8 | Max. 0.6 | 0.4-0.6 |
| New Si-Mo Alloy | 2.8-3.7 | 4.0-4.5 | Max. 0.3 | 0.8-1.0 |

In the new alloy, the silicon is increased to 4.5% to stabilize the ferrite matrix and to increase the strength while minimizing machinability issues. The oxidation resistance is also improved by the increase in silicon. Molybdenum was increased to 0.8% - 1.0%. Although high temperature tensile strengths and creep resistance may be increased by up to 2% Mo, the formation of shrinkage defects becomes more probable as Mo levels are increased beyond 1%.

Other elements, such as manganese and chromium, are restricted in the new Si-Mo alloy, to prevent the formation of pearlite. Decomposition of pearlite during thermal cycling can increase thermal stresses due to the expansion that accompanies graphite formation.

Fig. 4 illustrates the microstructures of the new and current alloys in the as-cast state. The microstructure of the current alloy consists of pearlite on the cell boundaries of a ferrite matrix [3]. The microstructure of the new alloy consists of cell-boundary eutectic Mo-carbides in a ferrite matrix. Additionally, a small amount of pearlite, promoted by the Mn in the alloy, is also present.

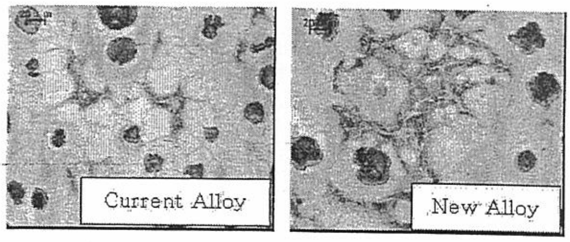

**Fig. 4 – The As-Cast Microstructures Of The Current And New Si-Mo Ductile Iron Alloys**

PHASE TRANSFORMATION

Silicon raises the critical temperature at which ferrite transforms to austenite. The critical temperature is considered to be the upper limit of the useful temperature range for exhaust manifold. Above this temperature, the expansion and contraction associated with the transformation of ferrite to austenite can cause distortion of the casting. This can also crack the protective surface oxide layer, reducing oxidation resistance.

The equilibrium $A_1$ temperature (calculated by the Thermo-Calc software) for the new Si-Mo alloy is 890°C (Fig. 5). As this figure shows, the percent of the ferrite (BCC) phase (Line 1) is about 90% when the temperature is below the equilibrium $A_1$ temperature. As the temperature increases above the equilibrium $A_1$ temperature, the percent of ferrite decreases sharply. However, under non-equilibrium conditions (like those measured by a dilatometer at 20°C/min heating rate, as shown Fig. 6), the $A_1$ transformation temperature starts at 870°C and finishes at 920°C. Additionally, as the heating rate of dynamo is increased greater than 20°C /min, transformation may be started over 870°C.

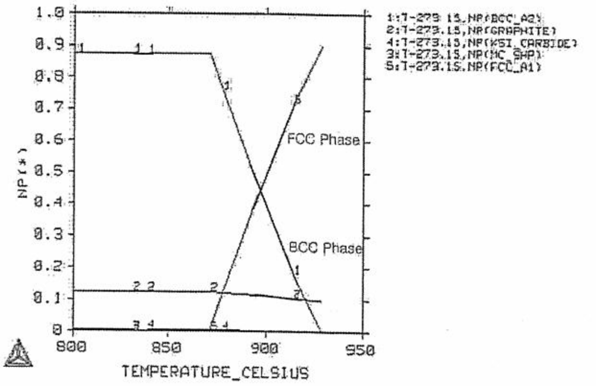

**Fig. 5 - The Calculated $A_1$ Temperature At Equilibrium For The New Si-Mo Ductile Iron Alloy (Note: NP(*) means percent of each phase.)**

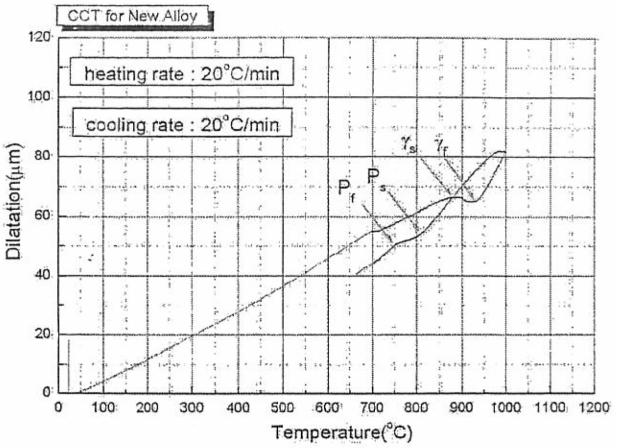

**Fig. 6 – The Measured $A_1$ Temperature Using A Dilatometer**

## HIGH TEMPERATURE OXIDATION

When pure iron oxidizes in air at high temperatures, it grows a scale consisting of layers of FeO, $Fe_3O_4$, and $Fe_2O_3$, and thus provides a good example of the formation of multi-layered scales. In the case of the Fe-Si alloy system, the oxides involved in this system include $SiO_2$, which forms the silicate $Fe_2SiO_4$ with FeO. At low silicon contents, $SiO_2$ is formed at the alloy surface. Simultaneously, it reacts with FeO to form *Fayalite*, $Fe_2SiO_4$, particles that are eventually engulfed by the scale [3].

To understand the oxidation resistance of the new alloy, high temperature oxidation tests were conducted in an air environment for 300 hours. The test results are shown in Fig. 7.

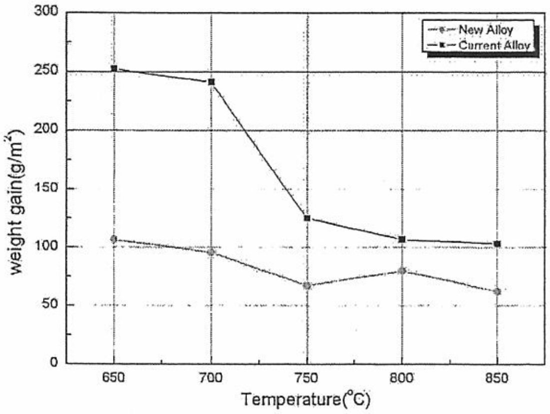

**Fig. 7 – The Weight Gain After Testing For 300 Hours At Elevated Temperatures**

As Fig. 7 show, the new alloy has a significantly lower ($115g/m^3$) weight gain (~50%) compared with the current alloy ($225g/m^3$) at temperatures below 700°C. Overall, Fig. 7 shows that the oxidation resistance of the new Si-Mo alloy is improved compared to the current Si-Mo alloy. Fig. 7 also shows that the weight gain (measured after 300 hours) decreases with increasing temperature above 700°C and reaches a minimum value 850°C.

This phenomenon of reduced weight gain can be explained by the following oxidation reactions:

$$2Fe + O2 = 2FeO \text{ ----- } \Delta G = -527{,}400+128.7T \tag{1}$$

$$C + O2 = CO2 \text{ ------ } \Delta G = -394{,}100-0.84T \tag{2}$$

$$2C + O2 = 2CO \text{ ------ } \Delta G = -223{,}400-175.3T \tag{3}$$

At high temperatures, oxidation of the carbon (decarburization) can occur as well as oxidation of the iron (reactions #2 and #3). If the weight loss by decarburization is greater than the weight gain by oxidation, the net weight is decreased.

Other oxidation reactions, such as the formation of $Fe_3O_4$ and $Fe_2O_3$, are ignored because of much greater mobility of ions in the FeO (wustite). Consequently this layer will be very thick compared with the magnetite ($Fe_3O_4$) and hematite ($Fe_2O_3$) layers. In fact, the relative thicknesses of FeO : $Fe_3O_4$ : $Fe_2O_3$ are in the ratio of roughly 95 : 4 : 1 at 1000°C [3].

To understand the high temperature oxidation of carbon and iron, the changes in the standard Gibbs-free energy at equilibrium state were determined for each reaction. Table 3 presents the results of these calculations.

**Table 3: Standard Gibbs-Free Energy Change Associated With An Increasing Temperature**

| Reaction | 650°C | 700°C | 850°C | Temp. Increase |
|---|---|---|---|---|
| (1) | -8.2E5 | -4.0E5 | -3.9E5 | \|ΔG\| decrease |
| (2) | -3.9E5 | -3.9E5 | -3.9E5 | Same |
| (3) | -3.8E5 | -3.9E5 | -4.0E5 | \|ΔG\| Increase |

With temperature increasing from 650 to 850°C, decarburization is more predominant than oxidation of iron. This can be seen as the increase in the absolute value of ΔG in reaction #3 and the decreases in ΔG in reaction #1 (Table 3.) Further, the diffusivity of carbon is faster than that of iron because carbon moves interstitially through the matrix.

Thus, the difference in weight gain at same temperature between the current Si-Mo alloy and the new Si-Mo alloy is caused by the added silicon content. As previously mentioned, if silicon is present in amounts greater than

4%, the $Fe_2SiO_4$ layer can be formed inside the FeO and prevent further oxidation of the iron.

The Rockwell Hardnesses of the two alloys were measured after the 300-hour oxidation tests at the various temperatures. The test results are shown in Fig. 8. The hardness value of new alloy is higher than that of current alloy at all temperature due to the added Si in solid solution and the precipitation of Mo-carbides. Hardness values slowly decrease as the temperature increases from 650 to 750°C due to the spheroidizing of the $Fe_3C$ in the pearlite. At 800°C, the hardnesses of both alloys decreased rapidly due to decomposition (or ferritization) of the $Fe_3C$ in pearlite. As the current alloy has a greater amount of pearlite compared to the new alloy, the decrease of hardness is greater in the current alloy.

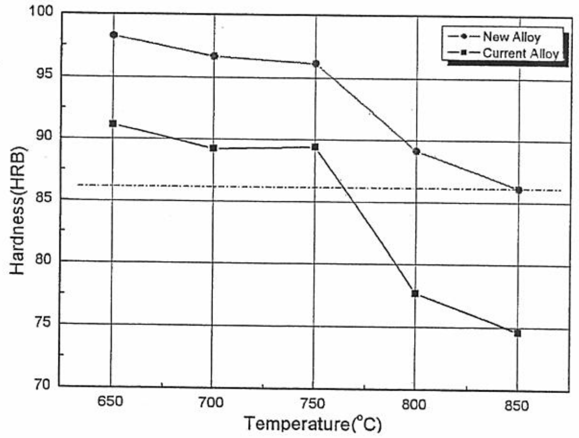

Fig. 8 - The Hardness Profiles After The 300-Hour Oxidation Tests

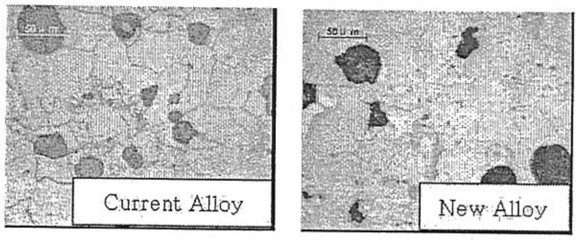

Fig. 9 – The Microstructures Of The Current And New Si-Mo Ductile Iron Alloys After Oxidation Testing At 800°C For 300 Hrs

Fig. 9 illustrates the microstructures of both the new and current alloys after oxidation testing at 800°C for 300 hours. Compared to the as-cast microstructure (Fig. 4), most of the pearlite in the cell boundary of the ferrite matrix has been decomposed after oxidation testing.

A review of the results in Fig. 8 shows that the critical hardness value needed to satisfy the specification (minimum HRB 86) is obtained at temperatures less than 760°C for the current alloy. However, in the case of the new alloys, the temperature can be as high as 850°C and the critical hardness value will still be met. These temperatures, the critical limit of the useful temperature range for exhaust manifolds, show the improved nature of the new Si-Mo alloy.

## THERMAL FATIGUE PROPERTIES

When exhaust manifolds are exposed to repeated thermal cycling during engine operations, thermal fatigue cracks can occur where there are stress-concentrating features, such as port-port junctions or sharply curved regions.

The crack initiation mechanism in ductile irons can be explained by the cracking of surface oxide scales due to different thermal expansions in different scales, or between the scale and the iron matrix. As the scale is repeatedly fractured by the thermal strains, continuous oxidation of the matrix occurs by as iron and oxygen ions easily interact. This phenomenon is called preferential oxidation. Thus, repeated cracking of the scale and preferential oxidation can create a notch, which can initiate a fatigue crack in the matrix. Further, preferential oxidation can also accelerate crack growth and shorten the time to final fracture. Fig. 10 illustrates an example of the initiation and growth of a thermal fatigue crack in a thick magnetite scale on 2%Cr-1%Mo steel [4].

Fig. 10 - Crack Initiation And Growth In A 2%Cr-1%Mo Steel By Alternate Rupturing Of Surface Oxide Layers [4]

If a similar mechanism is active in heat resistant ductile irons, then the thermal fatigue properties of ductile iron can be improved either by reducing the formation of weak oxide scales or through the formation of condensed oxide scales like $Cr_2O_3$ and $SiO_2$.

Additionally, the thermal fatigue properties of ductile iron can be improved by increasing tensile strength at high temperature. The tensile test results for the new and current alloys are compared in Fig. 11. As this figure shows, the tensile strength of the new alloy at 700°C does show improvement compared to the current alloy. The required strength criteria for the exhaust manifolds is a minimum of 70 MPa at the maximum operating temperature. As Fig. 11 shows, the new alloy can be used at temperatures up to a maximum of 800°C while the current alloy is restricted to 740°C.

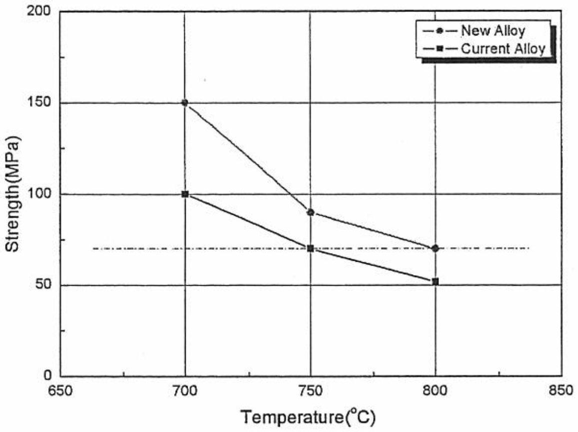

**Fig. 11 - Tensile Strength As A Function Of Temperature For The Current And New Si-Mo Ductile Iron Alloys**

Fig. 11 shows that, as the temperature increases, the tensile strengths of both the new and current alloys decrease. As mentioned previously, the new alloy is strengthened by Si in solid solution and by precipitation of Mo-carbides. At high temperatures, the effect of solid solution strengthening by silicon may almost disappear due to the increased solubility of silicon in iron. However, the new alloy still has good strength compared to the current alloy because the Mo-carbides are stable at the high temperatures. It is reported that decomposition of Mo-carbide may occur at temperatures over the $A_1$ temperature [5].

LCF Test Results

The low cycle fatigue tests were conducted at 700°C in strain control with a total strain range of $\Delta\varepsilon_t = \pm 0.1\% \sim \pm 0.5\%$. 700°C was chosen because the average temperature in a manifold exposed to exhaust gases is about 700 - 750°C. The strain rate was $1\times10^{-4}$ using a trapezoid wave and no hold time.

The strain rate of LCF was a similar with that of an actual exhaust manifold during dynamometer testing, calculated by time of thermal strain. And the hold time was eliminated because the test length would be significantly increased if the LCF tests were run at that strain rate with a hold time. That was an exact strain rate of an actual exhaust manifold during dynamometer testing.

The LCF test results are plotted in Fig. 12 as total strain range and number of cycles to failure. At ±0.3% total strain range, the fatigue life of new alloy is equal to that of current alloy. Above that strain range, the fatigue lives of new alloy and current alloy are meaningless values when it comes to exhaust manifold system. Because it is almost 80% constrained state and needs to be redesign to reduce the mechanical constraint. The thermal strain is maximum ±0.4% when it is heated to 700°C at free expansion state.

The fatigue life of the new alloy is longer than that of the current alloy at low strain ranges. And the deviations of fatigue life are much greater as the total stain ranges are lower.

These results can be explained by the fact that ductility is the predominant factor on fatigue life at high total strain range while strength is the predominant factor on fatigue life at low total strain range.

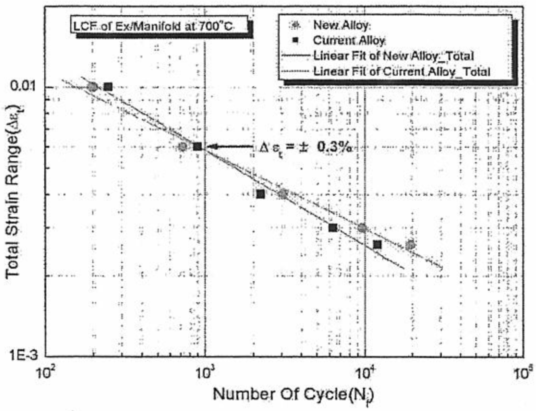

**Fig. 12 - Low Cycle Fatigue Test Results (T = 700°C)**

Generally thermal fatigue life is predicted by Coffin-Manson relationship, which relates plastic strain range and number of cycle to failure.

Coffin-Manson Relation: $\Delta\varepsilon_p = C\,(N_f)^{c}$

Fig. 13 illustrates the low cycle fatigue behavior of the new and current alloys as a function of plastic strain range. Both alloys satisfy the linear relationship between fatigue life and plastic strain range. As Fig. 13 shows, the two alloys have the same fatigue life at $\Delta\varepsilon_p = 0.0012$. Above that plastic strain range, the fatigue life of the new